The CRISPR Journal
Volume 1, Number 3, 2018
Mary Ann Liebert, Inc.
DOI: 10.1089/crispr.2017.0020

The CRISPR Journal

RESEARCH ARTICLE

TIE: A Method to Electroporate Long DNA Templates into Preimplantation Embryos for CRISPR-Cas9 Gene Editing

Hooman Bagheri,[1,2] Hana Friedman,[1–4] Harry Shao,[1] Yumaine Chong,[5] Chiu-An Lo,[6] Farida Emran,[6] Ibrahim Kays,[6] Xiang-Jiao Yang,[7] Ellis Cooper,[5] Brian E. Chen,[6] Katherine Siminovitch,[8] and Alan Peterson[1–4]

Abstract

Precise genome editing using CRISPR typically requires delivery of guide RNAs, Cas9 endonuclease, and DNA repair templates. Both microinjection and electroporation effectively deliver these components into mouse zygotes provided the DNA template is an oligonucleotide of only a few hundred base pairs. However, electroporation completely fails with longer double-stranded DNAs leaving microinjection as the only delivery option. Here, we overcome this limitation by first injecting all CRISPR components, including long plasmid-sized DNA templates, into the sub-zona pellucida space. There they are retained, supporting subsequent electroporation. We show that this simple and well-tolerated method achieves intracellular reagent concentrations sufficient to effect precise gene edits.

Introduction

Microinjection into the cytoplasm or pronuclei of mammalian zygotes is a well-established method for delivering all components required for CRISPR*-mediated genome editing.[1,2] Recently, zygote transfection by electroporation has gained favor due to technical simplicity, high throughput, and excellent embryo survival.[3–7] However, successful electroporation of double-stranded DNA and RNA longer than a few hundred nucleotides has been reported rarely.[8,9]

Zygotes and preimplantation embryos are surrounded by the zona pellucida (ZP), a thick acellular membrane composed of glycoprotein filaments. The ZP undergoes marked changes, including hardening following fertilization. Although it contains pores, some of which traverse its entire width, it remains semi-permeable, blocking passage of molecules based on size, composition, and configuration.[10,11] Notably, viruses do not cross the ZP but can infect zygotes when injected into the sub-ZP space.[12] Similarly, we show here that physically circumventing the ZP barrier permits electroporation of long DNA templates.

Electroporation protocols supporting transfection of CRISPR components and short oligonucleotide templates through the ZP typically include steps designed to increase ZP permeability.[3,4,13,14] Despite consistent success in delivering oligonucleotides by this method, electroporation of long DNA templates fails (Supplementary Table S1; Supplementary Data are available online at www.liebertpub.com/crispr). Moreover, as preimplantation embryos lacking a ZP have greatly diminished *in vivo* developmental potential,[15,16] removing their ZP is not an attractive solution. We therefore sought a means of breaching the ZP while maintaining its function and explored a two-step strategy in which CRISPR components are injected into the sub-ZP space prior to electroporation. Although attempted earlier for transgenic mouse production, this approach was only minimally

*Clustered Regularly Interspaced Short Palindromic Repeats.

[1]Laboratory of Developmental Biology, Departments of [2]Human Genetics, [3]Neurology and Neurosurgery, [4]Oncology, [5]Physiology and [7]Biochemistry, McGill University, Montreal, Quebec, Canada; [6]Centre for Research in Neuroscience, Research Institute of the McGill University Health Centre, Montreal, Quebec, Canada; [8]Lunenfeld-Tanenbaum Research Institute, Mount Sinai Hospital, Toronto, Ontario, Canada.

Address correspondence to: *Alan Peterson, Laboratory of Developmental Biology, Ludmer Building Rm. 328, McGill University, Montreal, Quebec, H3A 1A1 Canada,* E-mail: alan.peterson@mcgill.ca

effective.[17] In contrast, when implemented here for precise CRISPR editing, it met with success. We refer to this two-step strategy as TIE, designating Transfection by Injection and Electroporation.

Materials and Methods

Embryos

Zygotes and embryos were recovered from the reproductive tracts of CD1 and C57Bl/6 mice (Charles River Laboratories) following timed mating indicated by the presence of a copulation plug. C57Bl/6 BC5 mice (approximately 98% C57Bl/6 genotype) originally derived from chimeras bearing hybrid ES cells also were used. Zygotes were released from the fallopian tube by puncturing the ampulla, while later-stage embryos were expelled from the fallopian tube by flushing with Embryo Max M2 media (Millipore) using a syringe fitted with a short bevel 30G needle. Cumulus cells, when present, were removed by brief incubation at room temperature in Embryo Max M2 media with hyaluronidase (Millipore). Following recovery, embryos were transferred in batches to 60 mm Petri plates containing multiple 25 μL drops of Embryo Max Advanced KSOM Embryo Medium (Millipore) covered with 10 mL of mineral oil (M8410; Sigma–Aldrich). Plates were held in a humidified incubator at 37°C with 5% CO_2 in air overnight prior to introducing embryos and were maintained under the same conditions.

Sub-ZP injection

Small batches of embryos (typically <10) were transferred to an 85 μL drop of Opti-MEM 1 Reduced Serum Medium (Gibco) placed in the center of a 60 mm Petri plate overlaid with 10 mL of mineral oil. The Petri plate was moved to the stage of an inverted AXIO Observer A1 microscope (Zeiss) fitted with TransferMan NK2 micromanipulators (Eppendorf). Each embryo was picked up by a holding pipette controlled by a CellTram vario micrometer drive (Eppendorf), raised off the plate surface, and brought to the center of the field where the ZP was pierced by the injection pipette. Injection was controlled by a PLI-100A Pico-Liter Injector (Warner Instruments). Applied pressure and duration of the injection was regulated to achieve a discernable expansion of the ZP at injection; such parameters varied considerably, depending upon the size of the pipette orifice. When all embryos were injected (approximately 1 min per embryo), embryos were transferred, under a Stemi 2000 dissecting microscope (Zeiss), as a single row to the centre of a slide-mounted 6 cm long 3.2 mm gap electroporation chamber (BTX model #453) containing 700 μL of Opti-MEM at room temperature. In preliminary experiments, electroporation also was achieved using BTX model 610 cuvettes, as described for zygotes.[3] However, the slide-mounted chamber permits embryos to be oriented parallel to the electrodes, minimizing cell fusion and enhancing visualization post electroporation to facilitate embryo recovery. Electroporation pulses were delivered using a GenePulser equipped with X cell, CE, and PC modules (Bio-Rad Laboratories). Following electroporation, embryos were recovered, rinsed in Advanced KSOM, and transferred to 25 μL drops of Advanced KSOM under oil for culture. Notably, the voltage delivered varied somewhat from that set on the electroporator.

Imaging

Red fluorescent protein (RFP) encoded by the pENTR1A Ubi-mRFP-1 plasmid was detected using an inverted EVOS FL Auto fluorescence microscope (Life Technologies). Culture plates were transferred to the stage and embryo images were obtained at either 20× or 40× using transmitted and/or phase settings. RFP fluorescence was detected using the AMEP4655 Ex 585/29: Em 624/40 filter set. As nonspecific green fluorescent protein (GFP) fluorescence correlated with weak RFP signals, it was monitored using the AMEP4651 Ex 470/22: Em 510/42 filter set to confirm the RFP signal source.

Fluorescent signals from the Nanog-mCherry fusion protein and tagged ribonucleoprotein (RNP) and DNA were detected using an Axio Imager M1 Zeiss fluorescence microscope equipped with a X-cite series 120 Q light source and AxioCam MRm camera (Zeiss). Embryos were transferred to a drop of Advanced KSOM on a slide, cover-slipped, and placed on the stage where images at 20×, 40×, and 63× were obtained with white light and with filter set 38 Ex 470/40 Em 520/50 for GFP (nonspecific fluorescence) and filter set 20 Ex 546/12 Em 575/640 for reporter-encoded RFP.

DNA and RNP preparation

Plasmid DNA, pUbi-mRFP-1 (5.1 kb): The human ubiquitin C (*Ubc*) promoter and the mRFP-1 coding sequence followed by the bovine growth hormone (BGH) polyA site were cloned into pENTR1A (Invitrogen), as described.[18]

TracrRNA (Alt-R CRISPR-Cas9 tracrRNA, IDT) and each target-specific crRNA (Alt-R CRISPR-Cas9 crRNA, IDT) were re-suspended in TE, pH 7.5, at 100 μM. An equal volume of tracrRNA and a crRNA were combined and annealed by heating to 95°C for 5 min, followed by gradual cooling in a polymerase chain reaction (PCR) machine. This single-guide RNA (sgRNA) was aliquoted and stored at −80°C until use. To generate a RNP for sub-zona microinjection, *Streptococcus pyogenes* Cas9 nuclease (Alt-R S.p. Cas9 Nuclease 3NLS, IDT, or PNA Bio) and an sgRNA were diluted in equal volumes of TE (Tris

10 mM, EDTA 0.1 mM), pH 7.5, and Opti-MEM medium (Gibco, Thermo Fisher Scientific), combined, and incubated at room temperature for 20 min. Following this incubation, the DNA repair template was added. The solution was spun in the cold at 20,000 *g* for 15 min to remove particulates. The final concentrations in the injection solution used for HDR at the *Nanog* and *Rpl13a* loci were 48.7 ng/μL of Cas9 protein, 20 ng/μL of sgRNA, and 20 ng/μL of DNA repair template. For the RNP efficiency experiment assessed by MiSeq analysis, the final concentrations of reagents were 200 ng/μL of Cas9 and 100 ng/μL of sgRNA with or without 20 ng/μL of DNA repair template.

Alt-R™ CRISPR-Cas9 tracrRNA–ATTO™ 550 (IDT): ATTO™ 550 fluorescent dye was added to the 5′ end of Alt-R™ CRISPR-Cas9 tracrRNA (IDT). This form of tracrRNA can be used interchangeably with unlabeled Alt-R™ CRISPR-Cas9 tracrRNA (IDT) to generate sgRNAs and RNPs that are fluorescently labeled. Label IT® Plasmid Delivery Control, Cy®3 (Mirus) is a Cy®3-labeled circular plasmid DNA (2.7 kb).

Next-generation sequencing of blastocyst alleles

DNA from single blastocysts[19] was amplified with *Nanog*-specific primers containing a 22nt 5′ tag and Q5 polymerase (NEB) according to the manufacturer's instructions using these primers: CS1NanogNF3: 5′-ACA CTGACGACATGGTTCTACA TTGGAATGCTGCTC CGCTC and CS2NanogR4: 5′-TACGGTAGCAGAG ACTTGGTCT CCGACTGCTCTTCCGAAGG. Fifteen microliters of the 25 μL reaction was run on a gel for quality assurance and to estimate the product amount. The remaining PCR reaction from 104 blastocysts was delivered to the McGill University and Génome Québec Innovation Centre (Montréal, Canada) for barcode addition and MiSeq sequencing. A barcode and the Illumina i5 or i7 index were added to each amplicon by PCR using the Roche FastStart High Fidelity PCR system. Samples were normalized and pooled using a Perkin Elmer Janus liquid handler and purified with AMPure beads. Libraries were then quantified using the Quant-iT™ PicoGreen® dsDNA Assay Kit (Life Technologies) and the Kapa Illumina GA with Revised Primers-SYBR Fast Universal kit (Kapa Biosystems). Average fragment size was determined using a LabChip GX (PerkinElmer) instrument, and the samples were loaded on the MiSeq instrument with the MiSeq PE250 kit, as per Illumina directions. MiSeq data were analyzed using the Integrative Genomics Viewer.[20,21]

The Nanog-2A-mCherry repair template plasmid vector (9.7 kb)[1] was obtained from Addgene and the *Nanog* crRNA from IDT. The target sequence has been reported.[1]

The mRPL13A-PQR(V2)-RFP$_{nols}$ plasmid DNA template for the insertion of PQR(V2)-RFP$_{nols}$ into the endogenous *Rpl13a* locus has been reported.[22] The *Rpl13a* sgRNA target sequence was 5′-CCTTCCTCCGCCGCCAACTA. Integration of the *PQR-RFP* gene cassette into the endogenous *Rpl13a* locus was investigated by PCR.[19] DNA extracted from single blastocysts was amplified using a forward primer (CGGGTTGCTAACCTGGAATA) recognizing sequences outside the 5′ homology arm and a reverse primer (ACGAGCAGCTTTCTTCTCC) recognizing sequences within the *PQR-RFP* insert producing an amplicon of 2.5 kb. Two HDR templates were used, differing only by the presence of the RFP or mScarlet reporter (Addgene).

Results

Retention of DNA and Cas9-gRNA in the sub-ZP space

For TIE to be effective, CRISPR components injected into the sub-ZP space must be retained while embryos are introduced into the electroporation chamber. To evaluate their retention, we injected fluorescently tagged reagents in single or multiple boluses in volumes sufficient to distend the ZP. Within seconds, while the injection pipette still traversed the ZP, normal ZP diameter was restored. Following sub-ZP injection, a Cy3 labeled 2.7 kb plasmid was detectable by fluorescence microscopy throughout the sub-ZP space for at least 24 h (Fig. 1A, 1, 2, 5, and 6). Further, a sub-ZP signal remained after electroporation, demonstrating that the applied current did not eliminate sub-ZP retention. (Fig. 1A, 3 and 4).

Prior experiments in zygotes demonstrated that both Cas9 mRNA and Cas9 RNPs can be electroporated inward through the ZP.[3,4,14] To determine the extent of their retention within the sub-ZP space, we injected ATTO550-labeled RNPs composed of Cas9 and a 67 nt universal tracrRNA complexed with a 36 nt crRNA. Two hours later, a diffuse fluorescent signal and highly fluorescent puncta (indicative of RNP aggregates) were observed throughout the sub-ZP space (Fig. 1A, 7).

Embryo viability following plasmid transfection

Next, we determined if electroporation parameters capable of transfecting long DNA templates were compatible with embryo viability. A 5.1 kb circular plasmid bearing a Ubiquitin C promoted RFP reporter (pUbi-mRFP-1)[18] was injected sub-ZP into preimplantation embryos at different stages of development, and the appearance of RFP was monitored at 24 h for two- and eight-cell embryos and at 48 h for injected zygotes. Throughout, we used a common electroporation protocol shown to support transfection of CRISPR targeting reagents and short oligonucleotides presented on the outside of the ZP.[3,4,13,14] Single or multiple trains of seven square wave pulses,

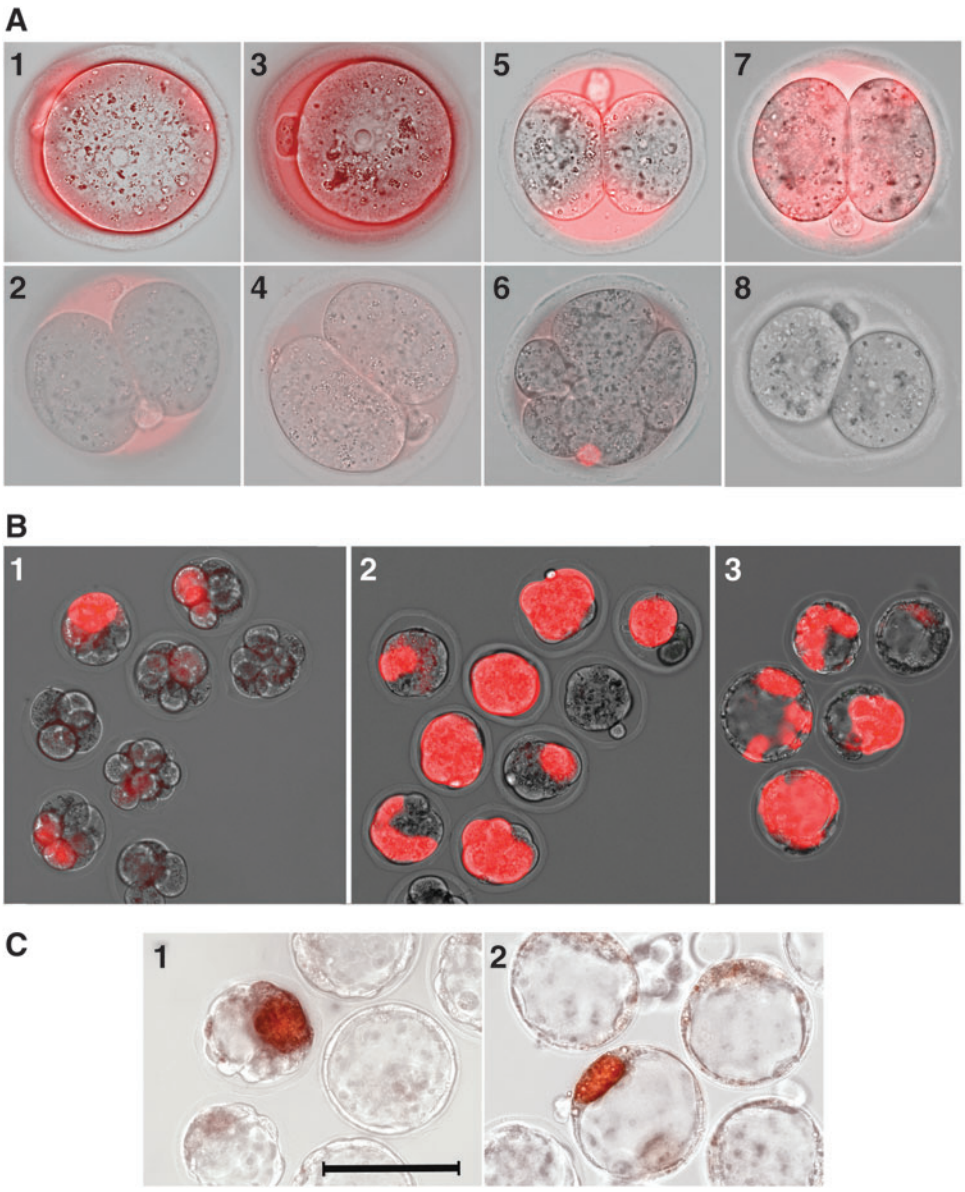

FIG. 1. **(A)** 1 and 5: Fluorescent signal 10 min after sub-zona pellucida (ZP) injection of Cy®3-labeled circular plasmid DNA (2.7 kb). 2 and 6: 24 h after sub-ZP injection of Cy®3-labeled plasmid. 3: 2 h after electroporation following sub-ZP injection of Cy®3-labeled plasmid. 4: 24 h after electroporation following sub-ZP injection of Cy®3-labeled plasmid. 7: 10 min after sub-ZP injection of Alt-R™ CRISPR-Cas9 tracrRNA–ATTO™ 550. 8: non-injected two-cell embryo control. **(B)** Groups of embryos were injected sub-ZP, electroporated, and cultured in the same media drop. 1: Expression of the pUbi-mRFP-1 reporter in E2 embryos; TIE as zygotes, three trains at 30 V/mm. 2: Expression in E2 embryos: TIE as 2-cell embryos, three trains at 25 V/mm. 3: E3 blastocysts TIE as eight-cell embryos, three trains at 25 V/mm. **(C)** 1 and 2: Fluorescence signal from Nanog-mCherry fusion protein detected in the inner cell mass of blastocysts subjected to TIE as 2-cell embryos. Calibration bar A = 67 μm, B = 145 μm, C = 100 μm.

each of 3 ms duration separated by approximately 5 s, were delivered at 1 KHz. Embryos electroporated at all developmental stages gave rise to brightly fluorescing cells (Fig. 1B, 1, 2, 3, and 4), although the effectiveness of different voltages and train numbers varied greatly. For example, for two-cell embryos, three trains at 18.75 V/mm were ineffective, three trains at 34.4 V/mm were poorly tolerated, while three trains at 25 V/mm led to transfection efficiencies between 20% and 100%. In contrast, at the eight-cell stage, where cell diameters

are reduced, three trains at 37.5 V/mm were well tolerated and effective (Supplementary Table S1).

While injection and electroporation of pUbi-mRFP-1 plasmid at concentrations ranging from 16.7 ng/μL to 4.35 μg/μL gave rise to embryos containing brightly fluorescing cells, embryo development often was delayed at high DNA concentrations, while lower concentrations supported greater cell division, leading to an increased number of fluorescing cells. Notably, the absolute sub-ZP DNA concentration following injection is difficult to define accurately. The ZP presents little impediment to small molecule diffusion,[10,23] and its rapid return to a normal diameter following injection likely results from trans-ZP expulsion of the injected solute but perhaps not the DNA templates it contains. Thus, the DNA concentration within the sub-ZP space may increase with the number of boluses (volume) delivered.

RNP transfection

To assess the effectiveness of RNP delivery by the TIE method, we investigated the frequency at which mutant alleles occurred in blastocysts derived from electroporated two-cell embryos. Amplicons spanning the single RNP target in the *Nanog* locus were analyzed for misrepair of double-strand breaks by next-generation sequencing with MiSeq PE250 technology—a strategy that reveals the full complement of alleles within the PCR product.

Three experiments were performed: two replicates in which embryos were exposed to a mixture containing RNP (200 ng/μL of Cas9 with 100 ng/μL of sgRNA) and HDR template (20 ng/μL), and one with RNP alone at 5× concentration. Note, in these experiments, we used RNP concentrations higher than those adopted for HDR. Of 98 blastocysts investigated, 36 (37%) revealed mutant alleles. Two involved insertions of 1 and 2 bp each, while the remainder were deletions ranging from 1 to 25 bp but typically of 3–6 bp. Twenty-four blastocysts carried a single mutant allele, while 12 revealed multiple alleles, and one presented with nine distinct variants. Thirty-eight percent (17/45) of the embryos transfected with 5× RNP alone bore one or more mutated alleles, while 28% (7/25) and 43% (12/28) of those transfected with the RNP and template bore mutations. Unexpectedly, the portion of mutant MiSeq reads was low in all mutation bearing blastocysts: 14 revealed mutant sequence in 1–5% of the reads, 16 in 6–14% of the reads, and six in ≥15% of the reads

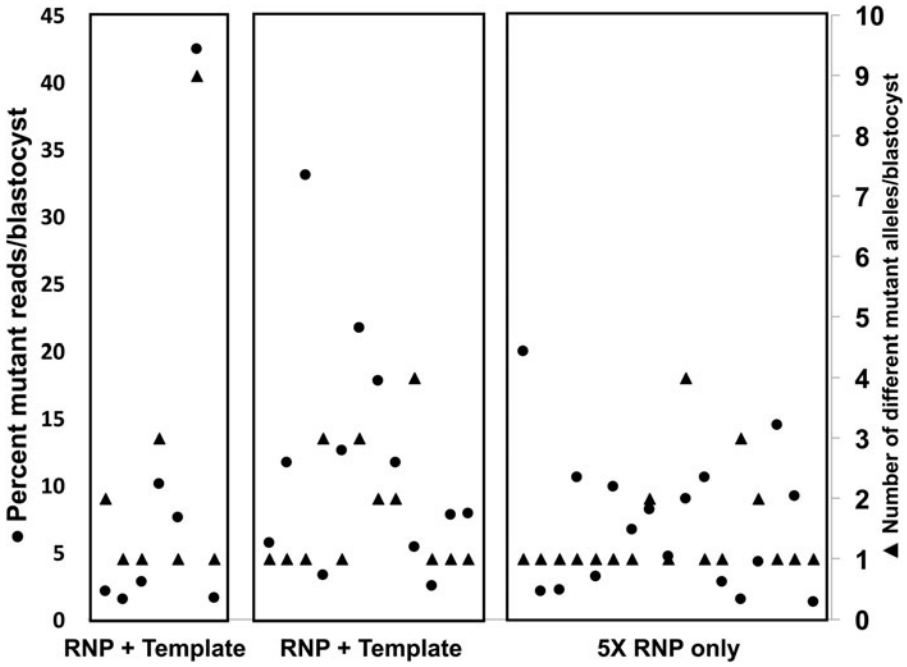

FIG. 2. Blastocysts electroporated with a *Nanog* targeting RNP at the two-cell stage were analyzed for mutations using MiSeq PE250 technology. Mutations at the gRNA target site were detected in 36/98 blastocysts. Each frame represents the mutation bearing blastocysts observed in one experiment. Solid dots indicate the percentage of mutant (vs. wild type) reads, while triangles represent the number of different mutant alleles carried by each blastocyst.

(Fig. 2). Notably, no correlation between RNP concentration and mutation frequency was apparent.

HDR following electroporation

Next, we determined if electroporation following injection of all CRISPR components into the sub-ZP space could yield sufficient intracellular reagent concentrations to support HDR. In two series of experiments, two-cell embryos were injected sub-ZP and subsequently electroporated with three trains ranging from 25 to 31.25 V/mm. First, we electroporated the RNP used in the above MiSeq experiments together with a 9.7 kb DNA repair template. Previously, when delivered by microinjection into zygotes, these *Nanog* targeting components were reported to support insertion in 9% of embryos surviving microinjection (75%) and result in an allele encoding a Nanog-mCherry fusion protein.[1] Nanog first accumulates in a subpopulation of cells in the inner cell mass (ICM), and 2/89 blastocysts subjected to TIE at the two-cell stage expressed a robust mCherry signal limited to the ICM (Fig. 1C, 1 and 2).

Next, we targeted the *Rpl13a* locus using an RNP and one of two 7.16 kb DNA templates designed to yield either mRFP or mScarlet Rp113a fluorescent proteins.[22] No fluorescent signal was detectable in the blastocysts derived from transfected two-cell embryos, but it is unknown if *Rpl13a* is robustly expressed during preimplantation development. Therefore, HDR was assayed by PCR[19] and the predicted insertion event was observed in 2/73 and 1/32 blastocysts transfected with the mRFP and mScarlet templates, respectively (Supplementary Fig. S1). Thus, sub-ZP injection and electroporation of mixes containing Cas9, gRNA, and DNA templates up to 9.7 kb supported precise CRISPR-mediated gene edits. In these experiments, sub-ZP injection and electroporation was well tolerated, with 90% (187/209) of the treated embryos developing to blastocysts.

Discussion

An increase in homology-directed repair (HDR) correlates with S phase in many cell types.[24] Therefore, introducing CRISPR components into advanced preimplantation embryos, where the cell cycle is foreshortened, might result in more frequent edits. However, when multicellular embryos were electroporated with the RFP reporter plasmid they typically demonstrated mosaic expression, suggesting that unequal transfection may counterbalance potential gains in HDR efficiency. Curiously, mosaic expression of the reporter plasmid was observed in embryos derived from electroporated pronuclear stage zygotes, demonstrating that subsequent expression underestimates actual transfection efficiency. Nonetheless, when electroporated at the two-cell stage, the HDR success rate at the *Nanog* locus was modest (2.3%) compared to previous reports (9%) using zygote microinjection.

Although the rate limiting step(s) in the method we describe have yet to be determined, the low abundance of mutant alleles detected in the MiSeq experiment suggests that RNP activity was suboptimal. All blastocysts carrying mutations exhibited extensive mosaicism, and 1/3 had more than one mutant allele. Notably, the frequency of mutant alleles detected by MiSeq is not a direct measure of RNP effectiveness. Many induced breaks are thought to undergo faithful repair, while in the continued presence of an effective RNP concentration, such restored targets should continue to be cleaved until mutation invalidates the sequence as a gRNA target.[25] The presence of mutations in 37% of the blastocysts analyzed by MiSeq suggests that successful RNP transfection was frequent. Assuming equivalent PCR amplification of wild-type and mutant alleles, multiple mechanisms might account for the low abundance of mutant alleles. The preassembled RNP used here differs from the *Cas9* mRNA and *Nanog* gRNA used previously to target the same site, and these may have different efficiencies. Successfully transfected cells could be at a developmental disadvantage, contributing few cells to the resulting blastocyst—a mechanism at odds with their apparently robust contribution to the ICM, as observed with HDR at the *Nanog* locus. Subsequent intracellular delivery of transfected RNP to the nucleus might be inefficient, and mutations introduced into only a few cells in later stage multicellular morula could limit their presence in blastocysts and underlie the observed mosaicism. The exceptional blastocyst bearing nine different alleles within 42% of its MiSeq reads requires that RNP induced non-homologous end joining occurred beyond the two-cell stage. To our knowledge, direct genotyping has not been performed previously on blastocysts developing from embryos transfected with CRISPR components. However, tissues (i.e., post ICM selection) of mice derived from microinjected zygotes also revealed extensive mosaicism and a striking number of different alleles.[26,27]

Conclusion

We show here that breaching the ZP barrier by direct injection of reagents into the sub-ZP space supports electroporation as an alternate method of transfecting zygotes and preimplantation embryos. Unlike direct injection into zygote cytoplasm or pronuclei, injection into the sub-ZP space requires minimal experimenter skill and is rapid and achievable with a wide range of pipette configurations. Electroporated zygotes and embryos demonstrate excellent survival, suggesting possible application in species where direct microinjection is less

well tolerated. The approach provides a simple means of delivering components into embryos throughout preimplantation development, including recently fertilized zygotes where mosaicism might be reduced[14] and later-stage embryos where HDR efficiency might be highest. Electroporation of late-stage embryos could also support the intentional derivation of mosaics for multiple experimental purposes.[28] As described here, the TIE method is likely amenable to optimization at many levels, including development of cell-specific electroporation programs, improved RNP solubility,[29] and possible separation of RNP and template delivery strategies to optimize each. Finally, direct delivery of diverse components into the sub-ZP space may facilitate their subsequent transfection into zygotes and preimplantation embryos using either traditional or emerging chemical transfection reagents.

Acknowledgments

This investigation was supported by CIHR grants to B.C., K.S., and A.P., and by a NeuroDevNet NCE grant to A.P. The authors wish to thank Dr. J.-F. Schmouth, J. Penny, and N. Saviuk for generous assistance in establishing the technique. The authors acknowledge the contributions of P. LePage and the McGill University and Genome Quebec Innovation Centre for the MiSeq procedure.

Author Disclosure Statement

No competing financial interests exist.

References

1. Yang H, Wang H, Shivalila CS, et al. One-step generation of mice carrying reporter and conditional alleles by CRISPR/Cas-mediated genome engineering. *Cell* 2013;154:1370–1379. DOI: 10.1016/j.cell.2013.08.022.
2. Li D, Qiu Z, Shao Y, et al. Heritable gene targeting in the mouse and rat using a CRISPR-Cas system. *Nat Biotechnol* 2013;31:681–683. DOI: 10.1038/nbt.2661.
3. Wang W, Kutny PM, Byers SL, et al. Delivery of Cas9 protein into mouse zygotes through a series of electroporation dramatically increased the efficiency of model creation. *J Genet Genom* 2016. DOI: 10.1016/j.jgg.2016.02.004.
4. Wang W, Zhang Y, Wang H. Generating mouse models using zygote electroporation of nucleases (ZEN) technology with high efficiency and throughput. *Methods Mol Biol* 2017;1605:219–230. DOI: 10.1007/978-1-4939-6988-3_15.
5. Chen S, Lee B, Lee AY, et al. Highly efficient mouse genome editing by CRISPR ribonucleoprotein electroporation of zygotes. *J Biol Chem* 2016;29:14457–14467. DOI: 10.1074/jbc.M116.733154.
6. Kaneko T. Genome editing in mouse and rat by electroporation. *Methods Mol Biol* 2017;1630:81–89. DOI: 10.1007/978-1-4939-7128-2_7.
7. Peterson A. CRISPR: express delivery to any DNA address. *Oral Dis* 2017;23:5–11. DOI: 10.1111/odi.12487.
8. Grabarek JB, Plusa B, Glover DM, et al. Efficient delivery of dsRNA into zona-enclosed mouse oocytes and preimplantation embryos by electroporation. *Genesis* 2002;32:269–276.
9. Peng H, Wu Y, Zhang Y. Efficient delivery of DNA and morpholinos into mouse preimplantation embryos by electroporation. *PLoS One* 2012;7:e43748. DOI: 10.1371/journal.pone.0043748.
10. Turner K, Horobin RW. Permeability of the mouse zona pellucida: a structure-staining-correlation model using coloured probes. *J Reprod Fertil* 1997;111:259–265.
11. Novo S, Barrios L, Ibanez E, et al. The zona pellucida porosity: three-dimensional reconstruction of four types of mouse oocyte zona pellucida using a dual beam microscope. *Microsc Microanal* 2012;18:1442–1449. DOI: 10.1017/s1431927612013487.
12. Liu C, Wang L, Li W, et al. Highly efficient generation of transgenic sheep by lentivirus accompanying the alteration of methylation status. *PLoS One* 2013;8:e54614. DOI: 10.1371/journal.pone.0054614.
13. Hashimoto M, Takemoto T. Electroporation enables the efficient mRNA delivery into the mouse zygotes and facilitates CRISPR/Cas9-based genome editing. *Sci Rep* 2015;5:11315. DOI: 10.1038/srep11315.
14. Hashimoto M, Yamashita Y, Takemoto T. Electroporation of Cas9 protein/sgRNA into early pronuclear zygotes generates non-mosaic mutants in the mouse. *Dev Biol* 2016;418:1–9. DOI: 10.1016/j.ydbio.2016.07.017.
15. Bronson RA, McLaren A. Transfer to the mouse oviduct of eggs with and without the zona pellucida. *J Reprod Fertil* 1970;22:129–137.
16. McLaren A. Transfer of zona-free mouse eggs to uterine foster mothers. *J Reprod Fertil* 1969;19:341–346.
17. Nemec LA, Skow LC, Goy JM, et al. Introduction of DNA into murine embryos by electroporation. *Theriogenology* 1989;31:233. DOI: 10.1016/0093-691X(89)90641-9.
18. Yurchenko E, Friedman H, Hay V, et al. Ubiquitous expression of mRFP-1 *in vivo* by site-directed transgenesis. *Transgen Res* 2007;16:29–40. DOI: 10.1007/s11248-006-9030-6.
19. Sakurai T, Watanabe S, Kamiyoshi A, et al. A single blastocyst assay optimized for detecting CRISPR/Cas9 system-induced indel mutations in mice. *BMC Biotechnol* 2014;14:69. DOI: 10.1186/1472-6750-14-69.
20. Thorvaldsdóttir H, Robinson JT, Mesirov JP. Integrative Genomics Viewer (IGV): high-performance genomics data visualization and exploration. *Brief Bioinform* 2013;14:178–192. DOI: 10.1093/bib/bbs017.
21. Robinson JT, Thorvaldsdottir H, Winckler W, et al. Integrative genomics viewer. *Nat Biotechnol* 2011;29:24–26. DOI: 10.1038/nbt.1754.
22. Lo CA, Kays I, Emran F, et al. Quantification of protein levels in single living cells. *Cell Rep* 2015;13:2634–2644. DOI: 10.1016/j.celrep.2015.11.048.
23. Sellens MH, Jenkinson EJ. Permeability of the mouse zona pellucida to immunoglobulin. *J Reprod Fertil* 1975;42:153–157.
24. Bee L, Fabris S, Cherubini R, et al. The efficiency of homologous recombination and non-homologous end joining systems in repairing double-strand breaks during cell cycle progression. *PLoS One* 2013;8:e69061. DOI: 10.1371/journal.pone.0069061.
25. Betermier M, Bertrand P, Lopez BS. Is non-homologous end-joining really an inherently error-prone process? *PLoS Genet* 2014;10:e1004086. DOI: 10.1371/journal.pgen.1004086.
26. Yen ST, Zhang M, Deng JM, et al. Somatic mosaicism and allele complexity induced by CRISPR/Cas9 RNA injections in mouse zygotes. *Dev Biol* 2014;393:3–9. DOI: 10.1016/j.ydbio.2014.06.017.
27. Yasue A, Kono H, Habuta M, et al. Relationship between somatic mosaicism of Pax6 mutation and variable developmental eye abnormalities-an analysis of CRISPR genome-edited mouse embryos. *Sci Rep* 2017;7:53. DOI: 10.1038/s41598-017-00088-w.
28. Mikuni T, Nishiyama J, Sun Y, et al. High-throughput, high-resolution mapping of protein localization in mammalian brain by *in vivo* genome editing. *Cell* 2016;165:1803–1817. DOI: 10.1016/j.cell.2016.04.044.
29. Burger A, Lindsay H, Felker A, et al. Maximizing mutagenesis with solubilized CRISPR-Cas9 ribonucleoprotein complexes. *Development* 2016;143:2025–2037. DOI: 10.1242/dev.134809.

Received for publication December 19, 2017;
Revised March 29, 2018;
Accepted May 7, 2018.